3-2-2018

Enhancing Clot Properties Through Fibrin-Specific Self-Cross-Linked PEG Side-Chain Microgels

Nicole Welsch
Georgia Institute of Technology

Ashley C. Brown
Georgia Institute of Technology

Thomas H. Barker
University of Virginia

L. Andrew Lyon
Chapman University, lyon@chapman.edu

Enhancing Clot Properties Through Fibrin-Specific Self-Cross-Linked PEG Side-Chain Microgels

Comments

Creative Commons License

Copyright

Accepted Manuscript

Title: Enhancing clot properties through fibrin-specific self-cross-linked PEG side-chain microgels

Authors: Nicole Welsch, Ashley C. Brown, Thomas H. Barker, L. Andrew Lyon
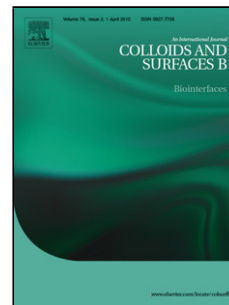
Please cite this article as: Nicole Welsch, Ashley C.Brown, Thomas H.Barker, L.Andrew Lyon, Enhancing clot properties through fibrin-specific self-cross-linked PEG side-chain microgels, Colloids and Surfaces B: Biointerfaces https://doi.org/10.1016/j.colsurfb.2018.03.003

Enhancing clot properties through fibrin-specific self-cross-linked PEG side-chain microgels

Nicole Welsch,[a] Ashley C. Brown[a,b,c], Thomas H. Barker[d], and L. Andrew Lyon[a,e*]

[a] School of Chemistry and Biochemistry, Georgia Institute of Technology, Atlanta, GA 30332, USA.

[b] Joint Department of Biomedical Engineering, North Carolina State University and The University of North Carolina – Chapel Hill, Raleigh, NC

[c] Comparative Medicine Institute, North Carolina State University, Raleigh, NC

[d] The Department of Biomedical Engineering, University of Virginia, Charlottesville, VA 22908 USA

[e] Schmid College of Science and Technology, Chapman University, Orange, CA 92866, USA

* Corresponding author

Email: lyon@chapman.edu (LAL)

Statistical summary:

7563 words, 6 figures, 0 tables

Graphical abstract
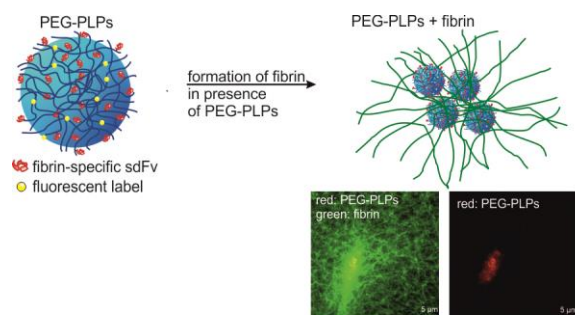
Graphical abstract: Scheme (top) and CLSM image (bottom) of polyethylene glycol-based platelet-like particles (PEG-PLPs) functionalized with variable domain-like recognition motifs (sdFvs) and their interaction with nascent fibrin fibers.

Highlights:

- Deformable PEG side-chain microgels with fibrin binding moieties (PEG-PLPs) were prepared
- PEG-PLPs adhere to nascent fibrin fibers and locally enhance the fiber density
- PEG-PLP-reinforced fibrin clots exhibit higher Young´s moduli than control clots
- PEG-PLPs improve the stability of fibrin clots against plasmin-induced fibrinolysis

Abstract

Excessive bleeding and resulting complications are a major cause of death in both trauma and surgical settings. Recently, there have been a number of investigations into the design of synthetic hemostatic agents with platelet-mimicking activity to effectively treat patients suffering from severe hemorrhage. We developed platelet-like particles from microgels composed of polymers carrying polyethylene glycol (PEG) side-chains and fibrin-targeting single domain variable fragment antibodies (PEG-PLPs). Comparable to natural platelets, PEG-PLPs were found to enhance the fibrin network formation *in vitro* through strong adhesion to the emerging fibrin clot and physical, non-covalent cross-linking of nascent fibrin fibers. Furthermore, the mechanical reinforcement of the fibrin mesh through the incorporation of particles into the network leads to a ~three-fold decrease of the overall clot permeability as compared to control clots. However, transport of biomolecules through the fibrin clots, such as peptides and larger proteins is not hindered by the presence of PEG-PLPs and the altered microstructure. Compared to control clots with an elastic modulus of 460 +/-260 Pa, PEG-PLP-reinforced fibrin clots exhibit higher degrees of stiffness as demonstrated by the significantly increased average Young´s modulus of 1770 +/±720 Pa, as measured by AFM force spectroscopy. Furthermore, *in vitro* degradation studies with plasmin demonstrate that fibrin clots formed in presence of PEG-PLPs withstand hydrolysis for 24 h, indicating enhanced stabilization against exogenous fibrinolysis. The entire set of data suggests that the designed platelet-like particles have high potential for use as hemostatic agents in emergency medicine and surgical settings.

Key words

Oligoethylene glycol-based microgels, platelet-like particles, fibrin clot, fibrin-targeting antibodies, elastic modulus, permeability

Introduction

Fibrin is the native provisional protein matrix that is formed from its precursor, fibrinogen, as part of the enzymatic cascade responsible for blood clotting. Along with platelet adhesion and the formation of a platelet plug, *in vivo* formation of the polymeric fibrin network is the key event in the arrest of bleeding at the site of injury (hemostasis).[1, 2] The fibrin gel serves as glue for activated platelets thereby reinforcing the platelet plug and ceasing bleeding. However, in cases of acute hemorrhage, these processes are insufficient and hemostatic technologies are used to aid the natural clotting cascade, reduce blood loss, and increase survival rates of patients suffering from traumatic injuries. Current technologies include topical dressings, such as polysaccharide-based agents and exothermic zeolites, recombinant clotting factors, and synthetic derived adhesives, *e.g.*, poly(cyanoacrylates) and *in situ* forming synthetic tissue sealants.[3-5]

Despite the growing number of available hemostatic agents, uncontrolled bleeding is still the leading cause of death due to trauma in battlefield and civilian settings.[6, 7]

In particular, treatment of non-compressible, internal injuries remains a major challenge. Cessation of internal bleeding is typically achieved by intravenous administration of antifibrinolytics and blood products, *e.g.*, coagulation factors and allogeneic platelets.[5, 8] More recently, synthetic-derived coagulation systems and, in particular, synthetic platelet substitutes, have been investigated as promising alternatives.[8-10] Synthetically derived hemostatic particles have many advantages as compared to blood-based transfusion products, since they could be more affordable, unlimited in supply, and easier in handling and storage. Most efforts have been focused on the development of surface-functionalized particles displaying platelet-binding motifs or platelet-cell surface adhesion motifs to facilitate platelet clustering and adhesion to the wound site.[9, 11]

 The chemistry as well as the physical properties of these systems, such as mechanical properties, particle size and shape, are very diverse which reflects the complexity of the development of "artificial platelets". Examples for these constructs are fibrinogen-coated microcapsules,[12] peptide-decorated liposomes,[13] nanoparticles consisting of a biodegradable copolymer core of poly(lactic-*co*-glycolic acid)/poly-(L)-lysine and poly(ethylene glycol) arms[14, 15], and discoidal shaped poly(allylamine hydrochloride)/bovine serum albumin layer-by-layer capsules[16]. In an alternative approach, Chan *et al.* developed a hemostatic polymer which induces hemostasis by cross-linking the fibrin matrix within clots.[17] These polymers mimic the function of the transglutaminase factor XIII and, in addition, bind specifically to fibrin monomers resulting in a hybrid polymer network with enhanced resistance to enzymatic degradation.

In our recent studies, we focused on the design of platelet-like particles (PLPs) which are able to recapitulate vital platelet functions that include binding, stabilization, and enhancement of fibrin clot formation under physiological flow.[18] For this purpose, micron-sized, ultralow cross-linked (ULC) poly(*N*-isopropylacrylamide-*co*-acrylic acid) (pNiPAm-*co*-AAc) microgels of unique deformability[19] were functionalized with variable domain-like recognition motifs (sdFv)[20] exhibiting high selectivity and affinity for nascent fibrin protofibrils but minimal binding to fibrinogen. These particles mimic the ability of natural platelets[21] to specifically bind to fibrin fibers and deform within the fibrin mesh to increase the number of microgel-fibrin binding events. These studies demonstrated that PLPs augment fibrin clotting, increase fibrin fiber density, and induce clot retraction *in vitro* similarly to natural platelets. The large network flexibility of PLPs was found to play a key role for complete clot collapse. Moreover, the purely synthetic particles achieve decreased bleeding times and blood loss *in vivo*, illustrating the utility of PLPs for use as synthetic hemostatic agents.

Herein, we demonstrate that PLPs can be designed from soft particle types other than ULC pNiPAm microgels. We used flexible self-cross-linked microgels based on the polymer poly(ethylene glycol) (PEG) to develop platelet-mimicking particles (PEG-PLPs). PEG polymers are generally considered to be biocompatible, low-toxic and bioinert and show minimal nonspecific protein binding.[22] Figure 1a and b display the constructs used for this study and their proposed interaction with nascent fibrin fibers. The particles are polymerized from oligo ethylene glycol methacrylate (OEGMA) and methacrylic acid in the absence of a cross-linking agent to form

negatively charged, self-cross-linked PEG side-chain microgel particles (scPEG

μgels). In our recent study we showed that scPEG μgels deform to a much greater

extent than particles cross-linked with poly(ethylene glycol) diacrylate (PEG-DA).[23]

Although scPEG μgels do not exhibit the same degree of network deformability as

ULC pNiPAm microgels, fibrin-PEG-PLPs were hypothesized to still recapitulate

important features of natural platelets. Therefore, scPEG μgels could be a good

alternative to the ULC pNiPAm microgels that were initially exploited as platelet

"body" for PLPs.[18] Conjugation of sdFv units to the polymer network was realized

via covalent coupling to the carboxylate groups of the microgels. The goal of our

investigation is to demonstrate the ability of PEG-based, fibrin-specific μgels to target

and enhance fibrin clot formation *in vitro* in a fashion that is similar to the results

reported in Ref.[18]. Furthermore we wish to explore differences of the physical

properties between native fibrin and microgel/fibrin composites with regards to the

mechanical stiffness as well as the permeability for the solvent and smaller

biomolecules. Finally, we study the degradability of microgel-reinforced fibrin gels *in*

vitro to analyze their stability against enzymatic hydrolysis as compared to native

fibrin networks.

Experimental

Materials

Chemicals were purchased from Sigma-Aldrich unless otherwise specified.

Olig(ethylene glycol) methyl ether methacrylate (M_n= 300, OEGMA$_{300}$) was passed

through a column of basic Al_2O_3 to remove the inhibitor prior to polymerization.

Methacrylic acid, methacryloxyethyl thiocarbomoyl rhodamine B (Poly Fluor 570,

Polysciences Inc.), potassium persulfate (KPS), (3-aminopropyl)-trimethoxysilane

(APTMS), and the covalent coupling reagents *N*-hydroxysulfosuccinimide (sulfo-

NHS) and *N*-(3-dimethylaminopropyl)-N-ethylcarbodiimide hydrochloride (EDC)

were used as received. Human fibrinogen (Enzyme Research Laboratories, FIB3,

plasminogen, von Willebrand factor, and fibronectin depleted), human αthrombin

(Enzyme Research Laboratories, HT 1002a), human plasmin (Enzyme Research

Laboratories, HPlasmin), *β*-D-glucosidase from almonds (Fluka), cytochrome c from

equine heart, and AlexaFluor 594 rabbit anti-goat Immunoglobulin G (Molecular

Probes, Inc.) were used without further purification. The following reagents were used

to prepare buffers: sodium phosphate monobasic monohydrate, sodium phosphate

dibasic heptahydrate (BDH chemicals), 2-(N-morpholino)ethanesulfonic acid (MES),

4-(2-hydroxyethyl)-piperazine-1-ethanesulfonic acid (HEPES), calcium chloride

(BDH Chemicals), sodium chloride, and sodium hydroxide. Acetone (BDH

Chemicals), isopropanol (BDH Chemicals), and ethanol (VWR) were used as

received. All water was distilled and deionized (Barnstead E-Pure) to a resistance of

18 MΩ. Additional particulate matter was removed using a 0.2 μm filter.

Particle synthesis

Self-cross-linked PEG-sidechain microgels were synthesized via surfactant-free

precipitation polymerization in a 250 mL three-necked round bottom flask equipped

with a reflux condenser, N_2 inlet, thermometer, and magnetic stirrer. OEGMA$_{300}$

(97.99 mol-%; 80.7 mM final concentration) was dissolved into 84 mL DI H_2O and the solution was degassed at room temperature by flushing with N_2 for 20 min while stirring. In the next step, the solution was heated to 80 °C in an oil bath and purged with N_2 while stirring at 450 rpm. Methacrylic acid (2 mol-%; 1.6 mM final concentration) dissolved in 0.5 mL DI H_2O and methacryloxyethyl thiocarbomoyl rhodamine B (0.01 mol-%; 9×10^{-3} mM final concentration) dissolved in 250 μL DMSO were added to the reaction solution and stirred for another 10 minutes. The reaction was started by addition of the initiator KPS (0.01 g dissolved in 1 mL DI H_2O; 0.4 mM final concentration). The polymerization was allowed to proceed for 6 hours at 80 °C under a N_2 blanket. After completion, the reaction solution was cooled to room temperature using an ice bath and filtered through glass wool to remove traces of coagulum. The final microgels were purified by dialysis (molecular weight cut off 12-14 kDa) against DI H_2O for two weeks and were lyophilized before use. The particle yield was ~80 % by mass.

Protein-conjugation to microgels

Fibrin-speficic sdFv (H6) and a random, non-binding clone (S11) were previously identified through phage-display biopanning. Production and characterization of sdFvs were performed as described in Ref.[18] The antibody fragments were conjugated to the carboxylate groups of the scPEG μgel using standard EDC/sulfo-NHS chemistry. Briefly, carboxylate groups on microgels were activated with 25 mM EDC and 37.5 mM sulfo-NHS in 0.1 M MES buffer, pH 5.5 for 20 minutes using a microgel concentration of 5 mg/mL. Microgels were centrifuged and the pelleted particles were

redispersed in 4 mg/mL sdFv solution (0.1 M phosphate buffer, pH 7.4). The

conjugation was allowed to proceed for 3 hours. Afterwards, the peptide-conjugated

particles were purified *via* dialysis against 10 mM HEPES, pH 7.4 at 4 °C for 2 days

(molecular weight cut off 100 kDa).

Particle characterization

Dynamic Light Scattering (DLS). DLS (DynaPro, Wyatt technology) was used to

determine the hydrodynamic radius (R_H) at 20 °C in 25 mM HEPES/150 mM NaCl,

pH 7.4. Buffer solutions were filtered through a syringe filter prior experiment (Supor

membrane, 0.2 μm pore width, PALL, Acrodisc). The scattering data was collected at

a scattering angle of 90° for 20 s per acquisition with a total of 25 acquisitions. The

measured intensity time correlation functions were analyzed using the cumulants

method to calculate the diffusion coefficient. From this value, R_H was determined

using the Stokes-Einstein equation.

Atomic Force Microscopy (AFM). The size and morphology of the microgels were

further characterized by AFM imaging of microgel particles adsorbed to a glass

substrate. Microgel monolayers were assembled on amine-functionalized glass cover

slips in accordance with Ref [23]. An MFP-3D AFM (Asylum Research, Santa

Barbara, CA) was used to image microgel monolayers in 25 mM HEPES/150 mM

NaCl, pH 7.4. Microgels were rehydrated by adding a droplet of buffer approximately

30 minutes before measurements to ensure equilibration. Conical-shaped silicon AFM

probes with Al reflex coating ($k = 42$ N m^{-1}) were mounted on an iDrive cantilever

holder and operated in-liquid and in AC mode. AFM data was processed using the supplied software written in an IgorPro environment (Wavemetrics, Inc.).

Tunable Resisitive Pulse Analysis. Particle size and size distribution was analyzed by translocation through nanopores (NP200) using a qNano (IZON Science, Oxford, UK) in 25 mM HEPES/150 mM NaCl buffer. All measurements were performed at 46.50 mm of applied stretch, 0.34 V, and 687 Pa. Particle diameters were calculated by using carboxylated polystyrene spheres (mean diameter = 212 nm) as calibration standard.

Fibrin gel preparation

Thrombin-initiated fibrin polymerization was performed at room temperature either on cleaned glass substrates (CLSM and AFM studies) or inside of a plastic capillary tube (Globe Scientific, Inc., I.D. = 0.75 mm, perfusion and fibrin degradation studies). Purified human fibrinogen, microgel particles, and human α-thrombin were mixed in 25 mM HEPES/150 mM NaCl/5 mM CaCl$_2$, pH 7.4 to initiate clot formation with final working concentrations of 5 mg/mL fibrinogen, 0.75 U/mL thrombin, and 0.75 mg/mL particles (control fibrin clots did not contain particles). The clots were allowed to polymerize for at least 1 h prior to experiments. Fibrin gels for CLSM studies were polymerized between a glass slide and a coverslip. To render fibrin clots fluorescent, labeled fibrinogen (AlexaFluor 488 conjugate, Molecular Probes, Inc.) was added to the mixture at a molar ratio of 1:50 labeled:unlabeled fibrinogen.

Confocal laser scanning microscopy (CLSM) of fibrin gels

Clots were imaged using a Zeiss LSM 510 Confocal Microscope using a 63x/1.4 NA oil DIC M27 objective. An Ar^+ laser at 488 nm and a HeNe laser at 543 nm were used for excitation of AlexaFluor 488 labeled fibrinogen and rhodamine labeled particles, respectively. The pinhole diameter was set to 1 airy unit and a resolution of 512 x 512 pixels for 8-bit images was chosen.

AFM force spectroscopy of fibrin gels

Fibrin clots were polymerized on glass coverslips for 30-45 minutes and then overlaid with 30 μL of either buffer solution or dispersion with 0.75 mg/mL PEG-PLPs or S11-scPEG μgels. The gels were incubated overnight in a humid environment. AFM nanoindentaion experiments were performed on a MFP-3D AFM (Asylum Research, Santa Barbara, CA) using a silicon nitride SPM sensor with a cantilever spring constant of 0.08 N m^1 and a 3.5 μm SiO_2 particle attached to it (NanoAndMore USA). The fibrin clots and colloidal probe were fully immersed in buffer solution. The inverse optical laser sensitivity (InvOLS) and spring constant of the AFM probe were calibrated by a combination of single force curves on a stiff glass substrate and thermal spectra using methods in the MFP-3D software. The AFM was operated in contact mode and force maps with scan sizes of 40 μm x 40 μm or 80 μm x 80 μm were collected as a 24 x 25 array of force curves with a trigger point set to 1.0 V. The stiffness of different points of the gels was determined by fitting the force-deformation curves to the Hertz model. In case of spherical indenter geometry, the Hertz model is described by

$$F = \frac{4}{3} \frac{R_c^{1/2}}{(1-v^2)} E \delta^{3/2} \qquad \text{Eq. 1}$$

where F is the force, R_c is the radius of the colloidal probe, v is the Poisson ratio, E is the elastic modulus, and δ is the deformation of the sample. Mean elastic moduli of different fibrin clots were calculated from force-indentation curves of at least 3 force maps for each construct.

Fibrin gel perfusion experiments

To measure the hydraulic permeability of the fibrin/microgel hybrid materials the gels were polymerized in transparent plastic tubes that are used as permeation chambers (Figure S1a). After polymerization, the fibrin gels were cut to a length ranging between 1 to 1.5 cm and connected to a reservoir containing 25mM HEPES/150 mM NaCl, pH 7.4 buffer solution. The buffer was perfused by gravity through the fibrin gel at different pressure gradients and the volumetric flow rate was calculated by tracking the air/buffer interface in the plastic tubing that has been connected to the end of the permeation chamber. Thereby, the pressure gradient was adjusted by the liquid height of the reservoir. The volumetric flow rate was measured at 5 different pressure gradients for 5 min (Figure S1b) and repeated 3 times for each condition. To visualize the flow through the clot and identify possible gel ruptures and detachments, the percolating buffer was supplemented with 0.02 mg/mL methylene blue. The permeability was calculated from Darcy´s law which is given by

$$Q = \frac{k}{\mu} A \frac{\Delta P}{L} \qquad \text{Eq. 2}$$

where Q is the volumetric flow, k is the Darcy constant, *i.e.*, the permeability constant, μ is the liquid viscosity, $\mathit{\Delta}P$ is the pressure gradient across the clot, and A and L are the cross-sectional area and the length of the cylindrical clot, respectively.

To study the porosity of the fibrin clots for biomolecules the diffusional transport of 4 proteins with molecular weights ranging from 12 000 to 340 000 g/mol was investigated. For this purpose, a protein mixture of cytochrome c (Cyt c, M_w ~ 12 300 g/mol), rhodamine-labeled immunoglobulin G (IgG, M_w ~ 150 000 g/mol), and AlexaFluor 488 conjugated fibrinogen (Fib, M_w ~ 340 000 g/mol) were prepared with final working concentrations of 0.1 mg/mL (Cyt c) and 0.033 mg/mL (IgG and Fib). A reservoir was filled with the solution of the protein mixture and connected to the fibrin gels. After perfusion for 45 minutes, the liquid within the fibrin gel was completely replaced by fresh protein solution, and ~ 50 μL of the solution that has passed the fibrin clots was collected to analyze the concentration of each protein after gel passage. Due to the distinct absorbance and fluorescence spectra of Cyt c, IgG, and Fib, it was possible to quantify each protein from the protein mixture simultaneously. In a separate experiment, transport of β-D-glucosidase with a concentration of 0.5 mg/mL (Glcase, M_w ~ 135 000 g/mol) was analyzed. The collected solution was tested for Glcase by using the quantitative CBQCA assay.

Clot degradation experiments

Fibrin clots formed in plastic capillary tubes were subjected to enzymatic degradation using human plasmin. Tubes were attached to a reservoir filled with 0.02 mg/mL plasmin and the volumetric flow rate through the clots was measured at certain time

points. Increased flow rates indicated progressing degradation of the fibrin network by plasmin.

Statistical analysis

All statistical analyses were performed with Prism software program (GraphPad, San Diego CA). Data was analyzed using a one-way analysis of variance (ANOVA) with a Tukey's posthoc test at a 95% confidence interval.

Results and Discussion

Preparation of fibrin-specific PEG-PLPs

For this investigation, rhodamine-labeled self-cross-linked microgels carrying PEG side-chains (scPEG μgels) and having a hydrodynamic diameter of 680 nm were prepared under cross-linker-free reaction conditions. Recently, we could show that it is possible to exploit chain transfer reactions originating from the oligo ethylene glycol side chains to create stable microgel particles with higher network flexibility than microgels containing a cross-linking monomer.[23] For example, when deposited on an amine-functionalized glass substrate, hydrated scPEG μgels spread with a diameter of 1031 ±107 nm but a small height of 106 ±27 nm (Figure 1c). Compared to PEG-DA cross-linked microgels, scPEG μgels have a diameter to height ratio that is ~ 3 times larger than that of cross-linked particles.[23]

Additionally, the elastic modulus of scPEG μgels were found to be <100 kPa and significantly smaller than the value found for cross-linked particles.[23] The soft

character of pNiPAm-based PLPs has been demonstrated to be essential to enable

multiple binding to fibrin, to form local areas with high fiber density, and finally to

induce overall clot retraction.[18] By analogy to our previous study, scPEG μgels were

rendered fibrin-specific by peptide conjugation of sdFvs that show high affinity for

nascent fibrin fibers but minimal binding to the soluble abundant precursor fibrinogen

(H6). Particles carrying non-binding antibody fragments (S11) were used as control

particles in addition to non-functionalized scPEG μgels. The recognition motifs have

been identified by phage display[24] and were thoroughly characterized in terms of

molecular weight and binding constants in Ref.[18]. Conjugation of peptides only

slightly decreased the mean size and porosity of the particles as shown by tunable

resistive pulse analysis (Figure S2). Thus, we can make the reasonable assumption that

the mechanical properties, *i.e.*, the deformability, of these particles are not altered

upon chemoligation of sdFvs.

Structural investigation of fibrin clots in presence of PEG-PLPs

To investigate the interaction of sdFv-conjugated scPEG μgels with fibrin, the

formation of a fibrin clot was initiated by thrombin in presence of H6-, S11- or

nonfunctionalized particles. Confocal microscopy images of these fibrin gels are

shown in Figure 2a-d. The images were taken 2 or 24 h post-polymerization.

Supplementation of the fibrinogen solution with fibrin-specific PEG-PLPs resulted in

highly heterogeneous fibrin network structures with local spots of high fiber density

(Figure 2c). It is important to note that these dense regions are found to be strongly

correlated with areas of high particle number density. The confocal images suggest

that interactions between nascent fibrin and particles result in the local coagulation of the PEG-PLPs. On the other hand, the presence of non-binding S11-scPEG μgels (Figure 2b) does not significantly modify the fibrin network structure at the particle concentrations used, since no differences to the native fibrin clot are discerned (Figure 2a). However, clots formed in the presence of unmodified particles were found to consist of a slightly more porous network compared to native fibrin (Figure 2d). Noteworthy, Douglas *et al.* analyzed the formation of fibrin-μgel constructs made of fibrinogen and ULC pNiPAm microgels at higher concentrations, 8 mg/L and 4 mg/L, respectively.[25] At these concentrations the μgels were found to form tubular-like networks of "pores" filled with μgel particles throughout the fibrin clot. On the other hand, no significant differences in the fibrin structure of fibrin were observed within μgel-free regions of the fibrin clot. The formation of these percolated colloidal networks were related to the fibrin polymerization kinetics rather to specific fiber–μgel and μgel–μgel interactions.[25] The studies shown here were conducted at lower concentrations, i.e. about five times lower microgel concentration and at a fibrinogen concentration of 5 mg/mL. Consequently, these two different findings demonstrate that both the concentration range of fibrinogen and the μgel suspension as well the chemical nature of the μgel will govern the overall structure of the fibrin-μgel composite. This point is addressed in more detail when we discuss the permeability studies of the fibrin networks.

We found that the number of areas with enhanced fibrin densities in samples containing PEG-PLPs increased over the time course of 24 h while the structure in the control samples remained essentially unchanged. This further indicates the dynamic

nature of the interactions between fibrin-binding PEG-PLPs and fibrin. This observation is comparable to features observed for PLPs based on ULC p(NiPAm-*co*-AAc) microgels although particle clustering is found to occur to larger extent in case of PEG-PLPs (Figure 2c, right top and bottom). Clot collapse in the presence of pNiPAm-based PLPs was explained by the ability of PLPs to serve as multiple bridging sites between adjacent fibrin fibers. Thereby, the extraordinary deformability of the microgel network allows each particle to maximize its binding to multiple fibers within the fibrin network. In case of PEG-PLPs lacking the same degree of particle softness, particle clustering induced *via* multivalent interactions to adjacent fibrin fibers might assist the formation of local collapsed fibrin structures.

Mechanics of fibrin clots in presence of microgels

To gain information on the network mechanical properties of the fibrin clots on the micrometer scale, AFM nanoindentation was employed in-liquid to generate elastic (E) modulus maps across the fibrin gels. To avoid any damage of the soft fibrin matrix, force-deformation curves were obtained using a soft cantilever with a colloidal probe attached to it. For these experiments, functionalized particles were added shortly after initiation of fibrin polymerization (30 min) to prevent binding and accumulation of scPEG μgels on the glass surface on which fibrin gels were formed. In this way, a more homogenous particle distribution throughout the fibrin clot, and, in particular, on the fibrin surface was guaranteed.

E-modulus maps of native fibrin and of fibrin clots containing PEG-PLPs and S11-scPEG μgels, respectively, are shown in Figure 3. Native fibrin clots formed from

fibrinogen concentrations equal or near that of human plasma are very soft, with low

strain shear moduli in the range of 140 to 350 Pa.[26] Thus, the average Young´s

modulus of the control clots (fibrin only) of 460 ±260 Pa corresponds well with

literature values. In contrast, fibrin clots prepared in presence of fibrin-binding PEG-

PLPs show large gradients of elastic moduli ranging from 700 to 4800 Pa reflecting

the highly heterogeneous network structure observed for these composites (Figure 3c).

The average Young´s modulus of these particle-enriched fibrin clots is calculated as

1770 ±720 Pa, which is 4 times larger than the value found for the control (fibrin only,

p <0.01). For comparison, clotting studies with platelet-poor and platelet-rich plasma

have demonstrated that platelets enhance the clot stiffness by a factor of ~10.[21, 27]

Thus, by analogy to platelets, binding of PEG-PLPs leads to reinforced fibrin networks

of higher stiffness and enhanced stability against mechanical disintegration. Further

studies suggest that the presence of non-binding S11-scPEG μgels show the tendency

to increase the mechanical properties of fibrin clots as well, although the overall fibrin

network morphology remains unchanged (Figure 2b and Figure 3c); for these

constructs an average elastic modulus of 960 ±130 Pa was found.However, this

observation is not surprising, since the microgels exhibit larger Young´s moduli than

fibrin and serve as space filling material for the pores within the fibrin network,

resulting in an overall stiffer and denser hybrid material.

Network permeability of fibrin clots

In addition to its role in mechanics, the fibrin network structure determines the fluid flow and solute transport into and out of a clot. To analyze the fluid flow, the hydraulic permeability of fibrin clots was quantified from Darcy´s law by analyzing the liquid flow rate through the clots at varying pressure gradients across the fibrin gels. Experiments with control fibrin gels gave comparable results to those reported previously.[28, 29] The permeability of fibrin clots polymerized from a solution of fibrinogen and PEG-PLPs is decreased about 3 times (Figure 4 a). Incorporation of non-binding S11-scPEG μgels into a fibrin clot also decreases the exchange rate of fluid. This observation is in accordance with the increased elastic moduli observed for particle-enriched fibrin gels and is explained by the microgels acting as space fillers for the pores within the fibrin mesh. The permeability data suggest that the mechanical reinforcement of the fibrin mesh through incorporation of the PEG-PLPs or S11-scPEG μgels into its pores is the main cause for the reduced permeability whereas the local PEG-PLP-induced fibrin collapse only contributes to a smaller extent. .

It is important to mention that scPEG μgels carrying no sdFvs at their periphery have an opposite effect on the network permeability (Figure 4b). Thereby, a linear relation is found between the particle concentration and Darcy constant; larger particle concentrations resulted in increased permeability (Figure 4b). This result is in accordance with the coarser fiber structure found in fibrin networks formed in presence of plain (unmodified) scPEG μgels. PEG is known to act as possible precipitant for proteins, including fibrinogen, which makes it a highly useful adjuvant for protein crystallization.[30-32] The origin of PEG induced precipitation might be explained by theories of attractive depletion and excluded volume, however, its

mechanism is not yet fully understood.[32, 33] Notably, the effectiveness of PEG in reducing the solubility of proteins increases with increasing size of the PEG chain and it was found that larger proteins, such as fibrinogen, tend to precipitate at lower PEG concentrations than smaller proteins. [31] Moreover, Sim et al. demonstrated that branched PEG molecules act as protein precipitants, although to lower efficiency than the linear homologues of equivalent molecular weights.[34]

From these studies, we can conclude that in analogy to linear PEG polymers, scPEG μgels are excluded from the fibrinogen surface and induce protein self-association as the microgel concentration is increased. We found that thrombin-initiated polymerization of fibrinogen in presence of scPEG μgels with concentrations ≥ 2 mg/mL results in the formation of fibrin networks consisting of a coarser structure and thicker fibers as compared to the control (fibrin only) (Figure S3). Moreover, these structures are similar to fibrin clots formed in presence of linear PEG polymers (Figure S4).

In the case of sdFv-conjugated scPEG μgels, fibrin-particle interactions become net attractive due to the presence of covalently bound sdFvs which specifically and strongly bind to fibrin fibers reversing the salting out effect of PEG. Thus, the interactions between PEG-PLPs and fibrin are thermodynamically favorable, which is suggested by the enhanced fiber density at areas with increased particle concentration. Furthermore, the addition of non-binding S11-scPEG µgels influences the fibrin network neither in a positive or negative way, with these particles acting only as space filling material. These findings show that these constructs have the potential to act as

platelet-substitutes, since the fluid flow (i.e., blood) through fibrin gels is greatly

diminished, possibly leading to reduced blood loss and bleeding times.

Fibrin clot degradation and protein transport

Lastly, we tested the ability of PEG-PLPs to increase the stability of fibrin clots

against fibrinolysis. Pre-formed fibrin clots were subjected to exogenous degradation

with plasmin using the setup established to characterize network permeability; fibrin

gels were connected to a reservoir filled with a solution of plasmin and the flow rate

through the gels was monitored at a constant pressure gradient as function of time. As

is clear from Figure 5a and b, the flow rate of control clots (fibrin only) increased

significantly after 100-500 minutes, which is related to gel rupture as a consequence of

fibrinolysis or complete clot degradation within this time period. In contrast, fibrin

clots formed in presence of PEG-PLPs withstand plasmin-catalyzed degradation for as

long as 24 h After 1 day of exposure to plasmin, the fibrin network containing PEG-

PLPs began to be hydrolyzed; complete digestion was observed within 48 h. This is an

important result since PEG-PLPs retard fibrinolysis in the beginning of hemostasis. In

a clinical application, one would expect this to lead to rapid clot formation and the

preservation of wound closure without impeding the wound healing process in later

stages.

It is important to note that fibrin gels polymerized in presence of S11-scPEG μgels

exhibit degradation rates comparable to the fibrin control. This observation suggests

that microgel particles partially occupying the voids in the fibrin network do not

significantly inhibit plasmin-induced hydrolysis. Two possible scenarios may explain the retarded fibrinolysis of PEG-PLP/fibrin assemblies: first, hindered transport of plasmin through the overall enhanced fibrin clot limits the attack of the enzyme to the outer regions of the fibrin clot facing the solution of plasmin; secondly, plasmin is able to penetrate the fibrin clot, however, fibrin-binding particles serving as additional cross-linking points of the fibrin network and multiple regions of enhanced fibrin fiber density impede the enzymatic hydrolysis of the gel.

To test our first hypothesis, we investigated the permeability of PEG-PLP/fibrin assemblies for proteins with varying molecular weights and sizes. For this experiment, we selected 4 proteins: cytochrome c (M_w = 12 300 g/mol, r = 1.8 nm)[35], AlexaFluor 594 labeled immunoglobulin IgG (M_w = 150 00 g/mol, r = 5.3 nm)[36], β-D-glucosidase (M_w = 135 000 g/mol, radius n. d.)[37], and AlexaFluor 488 fibrinogen (M_w = 340 000 g/mol, r = 10.7 nm)[38, 39] These proteins have Stokes radii that are smaller or larger than that of plasminogen A/B (inactive precursor of plasmin; M_w = 92 000/90 000 g/mol, Stokes radii = 4.3/4.5 nm[40]). Figure 6 shows the fractions of each protein type that passed through the PEG-PLP reinforced fibrin clot in comparison to the control (fibrin only). The concentration of cytochrome c, β-D-glucosidase, and IgG was unchanged for both clots indicating free passage of proteins with radii up to 6 nm. In contrast, in case of fibrinogen only a fraction of <10% was found to permeate the microgel/fibrin construct; however, this outcome was comparable to that observed for the control gel. It should be noted that the retention of fibrinogen by fibrin cannot be unambiguously ascribed to the size exclusion of the fibrin meshes for solutes with radii ≥10 nm, since binding between fibrinogen and

fibrin fibers *via* knob:hole interactions likely decreases the concentration of free fibrinogen in the solution.[41, 42]

Nonetheless, these experiments demonstrate that PEG-PLP/fibrin composites and control clots have comparable permeability for small biomolecules, suggesting that plasmin is able to freely diffuse through the fibrin network in presence of PEG-PLPs resulting in uniform degradation throughout the clot. Consequently, these findings strongly support our second hypothesis: free diffusion of small biomolecules, such as plasmin, is not impaired; however, PEG-PLPs strongly interact with fibrin and stabilize the fibrin network against plasmin-induced degradation by forming additional physical cross-links between fibrin fibers and by enhancing the fibrin network density. Additionally, transport of fibrin fragments out of the degrading clot is likely hindered by the presence of dense fibrin regions. This likely retards the hydrolysis of the fibrin network by plasmin. This is an important outcome since it suggests that PEG-PLPs could stabilize the fibrin clot in hemostasis and the early stages of the wound healing process without effecting the transport of important (bio)molecules through the clot.

Conclusions

The ultimate goal of this work was to design PLPs from soft colloidal particles and to analyze their effect on the morphological and (bio)physical properties of the fibrin clot *in vitro*. Self-cross-linked, PEG-side-chain microgels were rendered fibrin specific through chemoligation to sdFvs having fibrin binding constants in the nM range.[43] Strong adhesion between PEG-PLPs and fibrin results in the formation of dense fibrin regions distributed across the whole fibrin clot. The experimental data suggest fibrin-

induced particle coagulation leads to a synergistic effect between local fibrin network collapse and the increase of local particle number density. The alteration of the fibrin microstructure leads to a significant improvement of the robustness of microgel-enriched fibrin gels. This is demonstrated by the ~4 fold increase of the average Young´s modulus. Mechanical stabilization by PEG-PLPs is comparable to the stiffening effect observed in platelet-rich clots, although less pronounced. In addition, the physical cross-links established between the colloidal particles and fibrin network as well as the particle-induced formation of dense fibrin regions results in the enhanced stability against plasmin-induced fibrinolysis. This finding is very promising, since administration of PEG-PLPs might lead to longer lifetimes of the fibrin clot *in vivo* without the use of antifibrinolytic therapies.[27, 44] Moreover, we found that fluid flow through fibrin clots formed in presence of either PEG-PLPs or particles carrying non-specific antibody fragments, S11-scPEG μgels, is greatly diminished. From these findings we conclude that the reduced permeability is the consequence of the particles acting as space fillers for the voids in the fibrin network. The locally enhanced fibrin structures observed for gels formed in presence of PEG-PLPs only has a minor contribution. Althoughthe reinforcement of the fibrin clot by fibrin-specific PEG-PLPs delays clot degradation by plasmin, it does not limit the diffusion of biomolecules throughout the fibrin clot. This finding is very important with regards to the transport of crucial molecules participating in wound healing. In summary, this study highlights the platelet-mimetic activity of PEG-PLPs and the potential use of these systems as synthetic hemostats with application in emergency medicine.

Acknowledgements

Competing Interests Statement

The authors do not declare any competing interests.

References

[1] J.H. Levy, F. Szlam, K.A. Tanaka, R.M. Sniecienski, Fibrinogen and hemostasis: a primary hemostatic target for the management of acquired bleeding, Anesth. Analg. 114 (2012) 261-274.

[2] N. Laurens, P. Koolwijk, M.P. de Maat, Fibrin structure and wound healing, J. Thromb. Thrombolysis 4 (2006) 932-939.

[3] J.S. Boateng, K.H. Matthews, H.N.E. Stevens, G.M. Eccleston, Wound healing dressings and drug delivery systems: a review, J. Pharm. Sci. 97 (2008) 2892-2923.

[4] F. di Lena, Hemostatic polymers: the concept, state of the art and perspectives, J. Mater. Chem. B 2 (2014) 3567-3577.

[5] A.M. Behrens, M.J. Sikorski, P. Kofinas, Hemostatic strategies for traumatic and surgical bleeding, J. Biomed. Mater. Res., Part A 102A (2014) 4182-4194.

[6] J.A. Evans, W.K.J.P. van, D. McDougall, K.A. Lee, T. Lyons, Z.J. Balogh, Epidemiology of traumatic deaths: comprehensive population-based assessment, World J Surg 34 (2010) 158-63.

[7] E.G. Krug, G.K. Sharma, R. Lozano, The global burden of injuries, Am. J. Public Health 90 (2000) 523-526.

[8] M. Lashof-Sullivan, A. Shoffstall, E. Lavik, Intravenous hemostats: challenges in translation to patients, Nanoscale 5 (2013) 10719-10728.

[9] C.L. Modery-Pawlowski, L.L. Tian, V. Pan, K.R. McCrae, S. Mitragotri, A. Sen Gupta, Approaches to synthetic platelet analogs, Biomaterials 34 (2013) 526-541.

[10] S. Nandi, A.C. Brown, Platelet-mimetic strategies for modulating the wound environment and inflammatory responses, Exp. Biol. Med. 241 (2016) 1138-1148.

[11] M.J.R. Desborough, P.A. Smethurst, L.J. Estcourt, S.J. Stanworth, Alternatives to allogeneic platelet transfusion, Br. J. Haematol. 175 (2016) 381-392.

[12] M. Levi, P.W. Friederich, S. Middleton, P.G. De Groot, Y.P. Wu, R. Harris, B.J. Biemond, H.F.G. Heijnen, J. Levin, J. Wouter ten Cate, Fibrinogen-coated albumin microcapsules reduce bleeding in severely thrombocytopenic rabbits, Nat. Med. (N. Y.) 5 (1999) 107-111.

[13] M. Ravikumar, C.L. Modery, T.L. Wong, A. Sen Gupta, Peptide-Decorated Liposomes Promote Arrest and Aggregation of Activated Platelets under Flow on Vascular Injury Relevant Protein Surfaces in Vitro, Biomacromolecules 13 (2012) 1495-1502.

[14] J.P. Bertram, C.A. Williams, R. Robinson, S.S. Segal, N.T. Flynn, E.B. Lavik, Intravenous hemostat: nanotechnology to halt bleeding, Sci Transl Med 1 (2009) 11ra22.

[15] M.M. Lashof-Sullivan, E. Shoffstall, K.T. Atkins, N. Keane, C. Bir, P. Vande Vord, E.B. Lavik, Intravenously administered nanoparticles increase survival following blast trauma, Proc. Natl. Acad. Sci. U. S. A. 111 (2014) 10293-10298.

[16] A.C. Anselmo, C.L. Modery-Pawlowski, S. Menegatti, S. Kumar, D.R. Vogus, L.L. Tian, M. Chen, T.M. Squires, A. Sen Gupta, S. Mitragotri, Platelet-like Nanoparticles: Mimicking Shape, Flexibility, and Surface Biology of Platelets To Target Vascular Injuries, ACS Nano 8 (2014) 11243-11253.

[17] L.W. Chan, X. Wang, H. Wei, L.D. Pozzo, N.J. White, S.H. Pun, A synthetic fibrin cross-linking polymer for modulating clot properties and inducing hemostasis, Science Translational Medicine 7 (2015) 277ra29-277ra29.

[18] A.C. Brown, S.E. Stabenfeldt, B. Ahn, R.T. Hannan, K.S. Dhada, E.S. Herman, V. Stefanelli, N. Guzzetta, A. Alexeev, W.A. Lam, L.A. Lyon, T.H. Barker, Ultrasoft microgels displaying emergent platelet-like behaviours, Nat. Mater. 13 (2014) 1108-1114.

[19] H. Bachman, A.C. Brown, K.C. Clarke, K.S. Dhada, A. Douglas, C.E. Hansen, E. Herman, J.S. Hyatt, P. Kodlekere, Z. Meng, S. Saxena, M.W. Spears Jr, N. Welsch, L.A. Lyon, Ultrasoft, highly deformable microgels, Soft Matter 11 (2015) 2018-2028.

[20] V.L. Stefanelli, T.H. Barker, The evolution of fibrin-specific targeting strategies, Journal of Materials Chemistry B 3 (2015) 1177-1186.

[21] W.A. Lam, O. Chaudhuri, A. Crow, K.D. Webster, T.-D. Li, A. Kita, J. Huang, D.A. Fletcher, Mechanics and contraction dynamics of single platelets and implications for clot stiffening, Nat. Mater. 10 (2011) 61-66.

[22] J.M. Harris, R.B. Chess, Effect of pegylation on pharmaceuticals, Nat. Rev. Drug Discov. 2 (2003) 214-221.

[23] N. Welsch, L.A. Lyon, Oligo(ethylene glycol)-sidechain microgels prepared in absence of cross-linking agent: Polymerization, characterization and variation of particle deformability, PLoS One 12 (2017) e0181369.

[24] C.M. Lee, N. Iorno, F. Sierro, D. Christ, Selection of human antibody fragments by phage display, Nat. Prot. 2 (2007) 3001-3008.

[25] A.M. Douglas, A.A. Fragkopoulos, M.K. Gaines, L.A. Lyon, A. Fernandez-Nieves, T.H. Barker, Dynamic assembly of ultrasoft colloidal networks enables cell invasion within restrictive fibrillar polymers, Proceedings of the National Academy of Sciences 114 (2017) 885-890.

[26] J.P. Winer, S. Oake, P.A. Janmey, Non-linear elasticity of extracellular matrices enables contractile cells to communicate local position and orientation, PLoS One 4 (2009) e6382.

[27] J.L. Kristeller, B.P. Roslund, R.F. Stahl, Benefits and Risks of Aprotinin Use During Cardiac Surgery, Pharmacotherapy: The Journal of Human Pharmacology and Drug Therapy 28 (2008) 112-124.

[28] O.V. Kim, Z.L. Xu, E.D. Rosen, M.S. Alber, Fibrin Networks Regulate Protein Transport during Thrombus Development, PLoS Comp. Biol. 9 (2013).

[29] A.R. Wufsus, N.E. Macera, K.B. Neeves, The Hydraulic Permeability of Blood Clots as a Function of Fibrin and Platelet Density, Biophys. J. 104 (2013) 1812-1823.

[30] R. Bhat, S.N. Timasheff, Steric Exclusion Is the Principal Source of the Preferential Hydration of Proteins in the Presence of Polyethylene Glycols, Protein Sci. 1 (1992) 1133-1143.

[31] D.H. Atha, K.C. Ingham, Mechanism of Precipitation of Proteins by Polyethylene Glycols - Analysis in Terms of Excluded Volume, J. Biol. Chem. 256 (1981) 2108-2117.

[32] I.L. Shulgin, E. Ruckenstein, Preferential hydration and solubility of proteins in aqueous solutions of polyethylene glycol, Biophys. Chem. 120 (2006) 188-198.

[33] S.-L. Sim, T. He, A. Tscheliessnig, M. Mueller, R.B.H. Tan, A. Jungbauer, Protein precipitation by polyethylene glycol: A generalized model based on hydrodynamic radius, J. Biotechnol. 157 (2012) 315-319.

[34] S.-L. Sim, T. He, A. Tscheliessnig, M. Mueller, R.B.H. Tan, A. Jungbauer, Branched polyethylene glycol for protein precipitation, Biotechnol. Bioeng. 109 (2012) 736-746.

[35] D.K. Wilkins, S.B. Grimshaw, V. Receveur, C.M. Dobson, J.A. Jones, L.J. Smith, Hydrodynamic radii of native and denatured proteins measured by pulse field gradient NMR techniques, Biochemistry-Us 38 (1999) 16424-16431.

[36] J.K. Armstrong, R.B. Wenby, H.J. Meiselman, T.C. Fisher, The hydrodynamic radii of macromolecules and their effect on red blood cell aggregation, Biophys. J. 87 (2004) 4259-4270.

[37] A.K. Grover, D.D. Macmurchie, R.J. Cushley, Studies on Almond Emulsin Beta-D-Glucosidase .1. Isolation and Characterization of a Bifunctional Isoenzyme, Biochim. Biophys. Acta 482 (1977) 98-108.

[38] I. Axelsson, Characterization of Proteins and Other Macromolecules by Agarose-Gel Chromatography, J. Chromatogr. 152 (1978) 21-32.

[39] Z. Adamczyk, B. Cichocki, M.L. Ekiel-Jezewska, A. Slowicka, E. Wajnryb, M. Wasilewska, Fibrinogen conformations and charge in electrolyte solutions derived from DLS and dynamic viscosity measurements, J. Colloid Interface Sci. 385 (2012) 244-257.

[40] I. Sjoholm, B. Wiman, P. Wallen, Studies on Conformational-Changes of Plasminogen Induced during Activation to Plasmin and by 6-Aminohexanoic Acid, Eur. J. Biochem. 39 (1973) 471-479.

[41] J.W. Weisel, R.I. Litvinov, Mechanisms of fibrin polymerization and clinical implications, Blood 121 (2013) 1712-1719.

[42] A.S.C. Soon, C.S. Lee, T.H. Barker, Modulation of fibrin matrix properties via knob:hole affinity interactions using peptide-PEG conjugates, Biomaterials 32 (2011) 4406-4414.

[43] V.L. Stefanelli, T.H. Barker, The evolution of fibrin-specific targeting strategies, J. Mater. Chem. B (2015) Ahead of Print.

[44] D.T. Mangano, Y. Miao, A. Vuylsteke, L.C. Tudor, R. Juneja, D. Filipescu, A. Hoeft, M.L. Fontes, Z. Hillel, E. Ott, T. Titov, C. Dietzel, J. Levin, Mortality associated with aprotinin during 5 years following coronary artery bypass graft surgery, JAMA, J. Am. Med. Assoc. 297 (2007) 471-479.
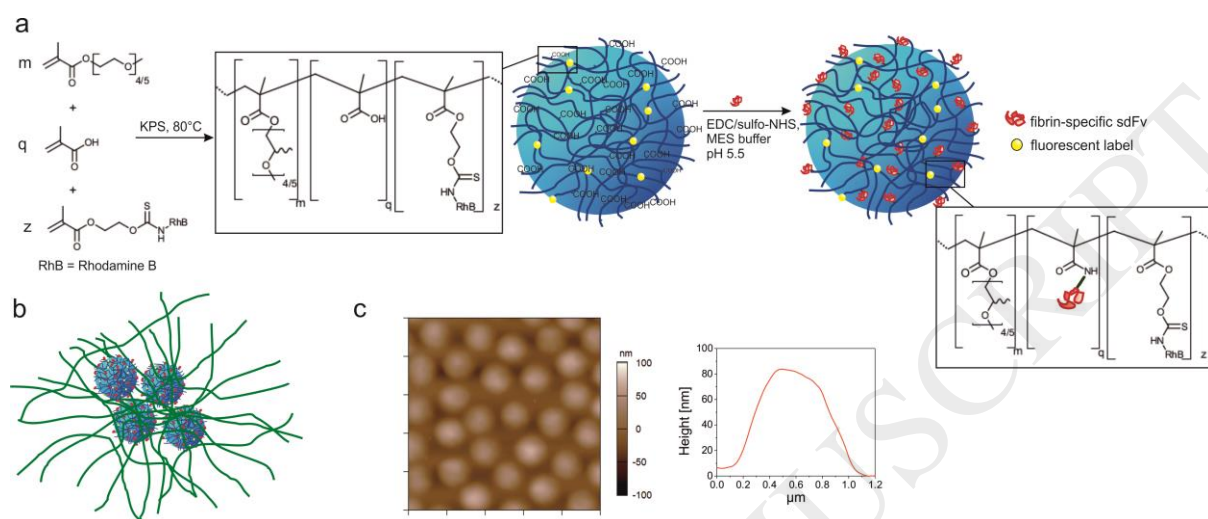
Figure captions

Figure 1 (a) Schematic representation of sdFv-functionalized scPEG μgels particles (PEG-PLPs) prepared from oligo ethylene glycol methacrylates containing 4 to 5 ethylene oxide repeating units and methacrylic acid . Particles were rendered fluorescent by copolymerization with methacryloxyethyl thiocarbomoyl rhodamine B. The antibody fragments were conjugated to the carboxylate groups of the scPEG μgel using standard EDC/sulfo-NHS chemistry. (b) Schematic of PEG-PLPs binding to nascent fibrin protofibrils. PEG-PLPs strongly adhere to fibrin fibers leading to an altered microstructure with locally enhanced fibrin fiber density. (c) AFM height retrace (left) and particle height profile (right) of scPEG μgels deposited on an amine-functionalized glass surface. The image has a scan size of 5 μm x 5 μm and was taken in 25 mM HEPES/150 mM NaCl, pH 7.4, i.e., the hydrated state of the particles.
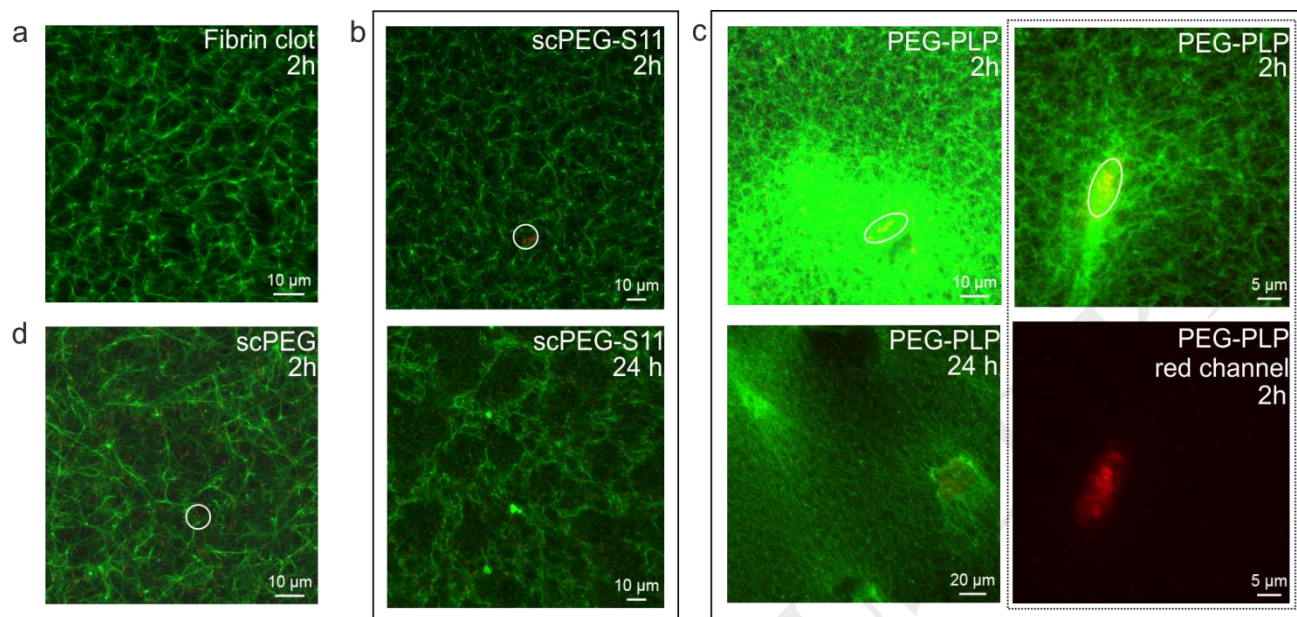
Figure 2 CLSM images of fibrin clots polymerized without particles (a), in presence of S11-conjugated scPEG μgels (b), PEG-PLPs (c), and unmodified particles (d) taken 2 or 24 h post-polymerization. Fibrin (green), particles (red). Circles highlight positions in the clot containing both fibrin fibers and particles. The red channel in panel (c) (bottom right) highlights particle clustering induced by multivalent interactions to adjacent fibrin fibers.
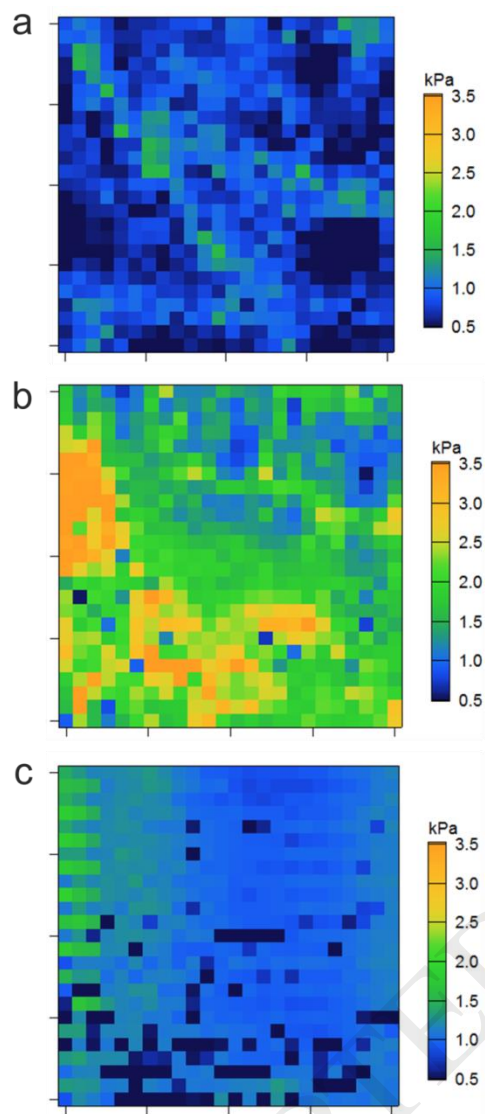
Figure 3 E-modulus maps of native fibrin (a) and fibrin clots formed in presence of PEG-PLPs (b) and S11-scPEG µgels (c). Each map has a scan size of 40 µm x 40 µm.
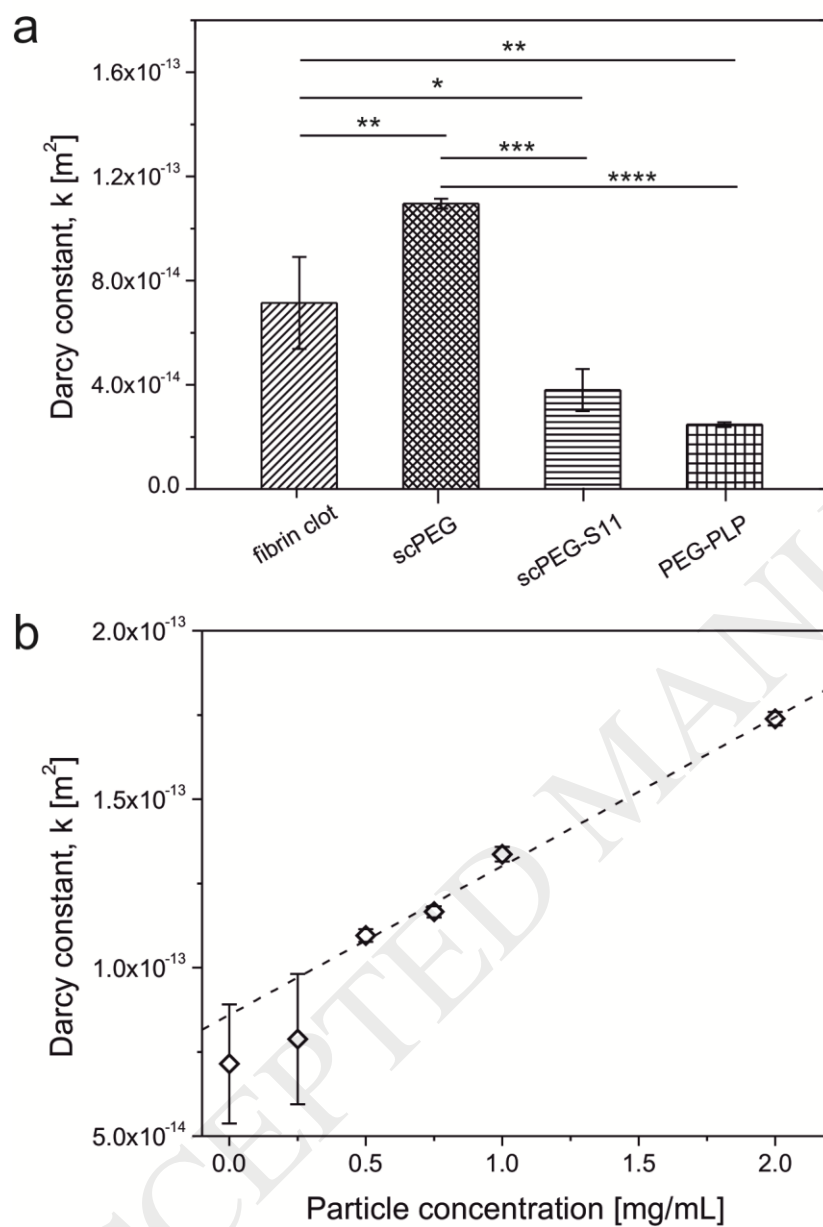
Figure 4 (a) Permeability constants of fibrin clots formed in absence or presence of fibrin-binding PEG-PLPs, non-binding S11- and unfunctionalized scPEG µgels (* p <0.05, ** p <0.01, *** p <0.001, **** p <0.0001). (b) Dependence of the Darcy constant of fibrin gels on the concentration of unmodified scPEG µgel added during clot formation. Error bars represent the standard deviation of the mean calculated from a total set of n=3 measurements.
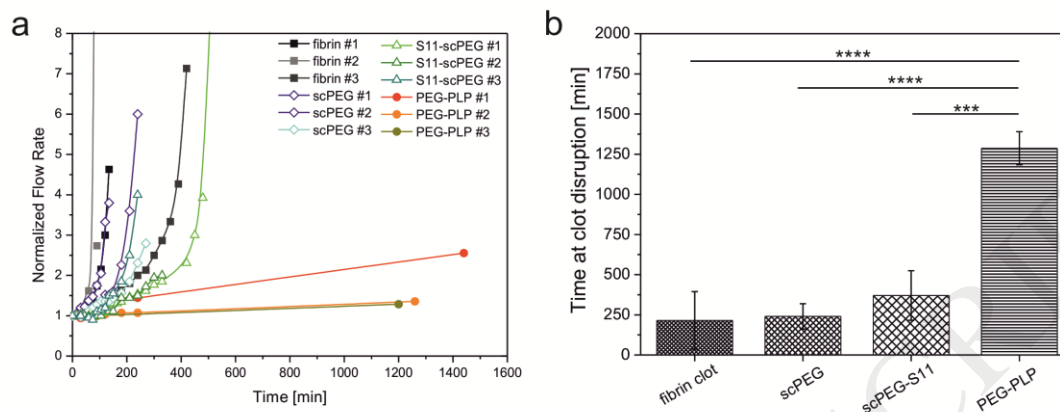
Figure 5 (a) Time-dependent degradation of fibrin clots formed in presence of S11-scPEG μgels and PEG-PLPs as measured by the flow rate through the degrading gels. The control is a fibrin clot formed in absence of particles. Flow rates were normalized to the flow rates of the clots before initiation of degradation by plasmin.(b) Time point at clot disruption. This time point is defined as the time at which the fibrin clot loses contact to the inner walls of the capillary leading to a drastic increase of the flow rate. In case of fibrin gels containing PEG-PLPs the presented data represents the last data points where the gels were still intact (*** $p < 0.001$, **** $p < 0.0001$). Errors bars represent the standard deviation of the mean calculated from a total set of n=3 measurements.
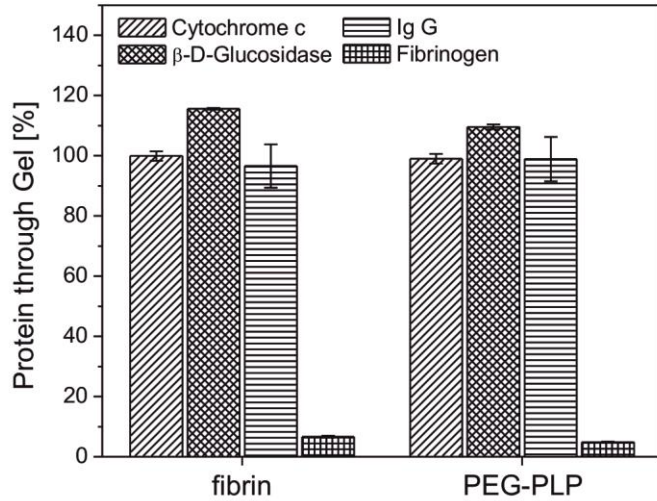
Figure 6 Fraction of cytochrome c, IgG, β-D-glucosidase, and fibrinogen passed through a fibrin clot

formed in absence and presence of PEG-PLPs. Experiments were performed at constant pressure

gradient, i.e., flow rate. Errors bars represent the standard deviation of the mean calculated from a

total set of n=3 measurements.